Lipids (2014) 49:203–206
DOI 10.1007/s11745-013-3845-8

COMMUNICATION

The β-Subunit of Cholera Toxin has a High Affinity for Ganglioside GM1 Embedded into Solid Supported Lipid Membranes with a Lipid Raft-Like Composition

G. Margheri · R. D'Agostino · S. Trigari · S. Sottini · M. Del Rosso

Received: 10 June 2013 / Accepted: 13 September 2013 / Published online: 11 October 2013

Abstract In this communication, we report on the fabrication of GM1-rich solid-supported bilayer lipid membranes (ssBLM) made of sphingomyelin and cholesterol, the main components of lipid rafts, which are the physiological hosting microenvironment of GM1 on the cell membrane. The functionality of the ganglioside has been checked by measuring the apparent dissociation constant K_D of the complex formed by the β-subunit of the cholera toxin and GM1. The value found deviates less than one order of magnitude from that measured for in vivo cells, indicating the potential of these ssBLM as optimized in vitro biomimetic platforms.

Keywords Lipid rafts · Gangliosides · Surface plasmon resonance

Abbreviations

C	Cholesterol
CTB	β-Subunit of the cholera toxin
DOPC	1,2-Dioleoyl-*sn*-glycero-3-phosphocholine
HBS	HEPES buffer solution
POPC	1-Palmitoyl-2-oleoyl-*sn*-glycero-3-phosphocholine
CerPCho	Brain sphingomyelin
SPR	Surface plasmon resonance
ssBLM	Solid supported lipid bilayer membrane
SUV	Small unilamellar vesicle

Electronic supplementary material The online version of this article (doi:10.1007/s11745-013-3845-8) contains supplementary material, which is available to authorized users.

G. Margheri (✉) · S. Trigari · S. Sottini
Institute for Complex Systems, National Research Council, Via Madonna del Piano 10, 50019 Sesto Fiorentino, Florence, Italy
e-mail: giancarlo.margheri@isc.cnr.it

R. D'Agostino · M. Del Rosso
Department of Pathology and Experimental Oncology, University of Florence, Viale G.B. Morgagni 50, 50134 Florence, Italy

Introduction

Ganglioside GM1 is an important effector responsible for many important cellular functions [1, 2]. It is mainly resident in the lipid-ordered regions of the cell membrane rich in CerPCho and C called lipid rafts, whose environmental effects may have important pharmacological implications on the molecular functional properties [3–6]. In order to best replicate the ganglioside functionality, its inglobation in artificial BLM biomembranes composed by CerPCho and C is thus a necessary prerequisite. So far, GM1-enriched BLM have been fabricated in the form of unilamellar vesicles [7, 8], but there is very little in the literature reporting on the formation and behavior of GM1-rich CerPCho/C BLM fabricated on solid-supports. In particular, the solid-supported bilayer lipid membranes (ssBLM) morphological structure, and the ganglioside organization have been locally investigated via atomic force microscopy and fluorescence microscopy [9, 10], but important properties of GM1, such as the binding affinity, could not be achieved with such tools. Recently, the SPR technique was exploited to recognize the presence of GM1 in GM1/CerPCho/C domains demixed from GM1/DOPC/CerPCho/C biomembranes via the binding of the ganglioside with the β-subunit of the cholera toxin (CTB) [11], but the analysis was restricted to the evaluation of the GM1–CTB association rates. In this work we built artificial GM1/CerPCho/C regions above plasmonic transducers. As in [11], the presence of GM1 was detected via its association

with CTB but, in addition to the association rates, here we also measured the dissociation constant of the complex CTB–GM1 and the consequent apparent K_D, gaining insight into the functionality of this important ganglioside when resident in a physiological-like environment.

Materials and Methods

The ssBLM:GM1 were assembled by exploiting the fusion of small unilamellar vesicles (SUV) on a SiO_2 interface, using the same procedure described in our recent paper on the fabrication of ssBLM:GM3 [12]. The plasmonic transducers were fabricated accordingly.

The stock solutions for the preparation of GM1/CerPCho/C mixtures were obtained in the same way as that used to obtain GM3/CerPCho/C mixtures described in [12]. The resulting ssBLM had the molar composition $GM1_x$CerPCho$_{0.6\ -\ x}C_{0.4}$ with $x = 0, 0.02, 0.05, 0.1, 0.2$ corresponding to 2, 5, 10, 20 mol% GM1 concentration. In the tests reported here, five CTB solutions (4.1, 8.3, 12, 24.5, 35 nM) were generated starting from a stock solution of CTB obtained by dissolving 2 μg of CTB (Sigma Aldrich) in 2 mL HBS.

The SPR spectrometer is a home made instrument described in [12]. For the convenience of the readers we briefly list the measurements steps:

1. Injection of $GM1_x$CerPCho$_{0.6\ -\ x}C_{0.4}$ SUV solution in the reaction cell and recording of a first SPR spectrum. The plasma angle θ_a (corresponding to the minimum reflectivity) is obtained (Fig. 1 ESM).
2. Recording of the SUV fusion on SiO_2 kinetic at the reflectivity setpoint of 0.3 until stabilization occurs.
3. Rinsing three times with HBS and recording of a new SPR spectrum. The plasma angle θ_b is obtained.
4. Resetting the reflectivity setpoint to 0.3 and inject the CTB solution.
5. Recording of the CTB association kinetic until the steady state is reached.
6. Rinsing three times and recording of the SPR spectrum. The plasma angle θ_c is obtained.
7. Repetition of these steps with GM1-free ssBLM and 35 nM CTB solution.
8. Elimination of the SUV solution from the cell and filling it with HBS, in order to record the CTB dissociation kinetics in the case of [GM1] = 10 mol%.

Results and Discussion

GM1-enriched ssBLM were successfully obtained via SUV fusion with homogeneity and stability similar to those documented in [12] for the fabrication of ssBLM:GM3.

Our SPR measurements indicate a ssBLM thickness of 6.3 nm, that is consistent with a partial filling with GM1 [10], but too close to that, 6.1 nm, measured for pure CerPCho ssBLM [13] to assume that it is a conclusive proof of the enrichment. Thus, the GM1 presence has been inferred more directly via binding tests performed in the presence of CTB, the specific ligand of GM1, put in contact with GM1-rich and GM1-free ssBLM. In the case of GM1-free ssBLM, no significant spectrum shift was found upon CTB addition, indicating that GM1 was selectively recognized. In all the tests, the unaltered shape of the SPR spectra, as visible in the example shown in Fig. 1 ESM, shows good stability and uniformity of the ssBLM in the various processing stages. The measurement of the GM1–CTB dissociation constant was carried out using samples of $GM1_{0.1}$CerPCho $_{0.5}C_{0.4}$ ssBLM, and CTB solutions at the concentrations indicated in "Materials and Methods". The shifts of $\Delta\theta_{CTB} = \theta_c - \theta_b$ vs CTB concentration are reported in Fig. 1. The data were fitted to a Langmuir isotherm and the value of $K_D = (1.5 \pm 0.5)$ nM was calculated for the apparent dissociation constant. This is, to our knowledge, the first measurement of the binding strength of the complex GM1–CTB when GM1 is hosted in a CerPCho/C ssBLM.

Since this measurement has 33 % of uncertainty, we thought it is appropriate to measure K_D also by recording the association and dissociation kinetics (Fig. 2a, c respectively). The predicted linear trend of the fast association rate constant k_{on} with CTB concentration [14] is confirmed in Fig. 2b. Its linear best fit gives a value of $k_{ass} = (1.10 \pm 0.04) \times 10^5\ M^{-1}s^{-1}$, while the average

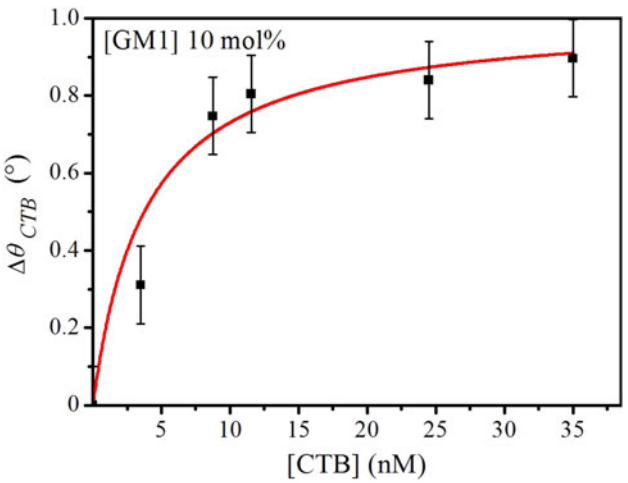

Fig. 1 Experimental shifts of the resonance angle (*squares*) vs CTB concentration, corresponding to GM1–CTB binding at [GM1] = 10 mol%. The line (*red* only in the online version) is the best fit of the data to a Langmuir isotherm, that corresponds to a dissociation constant $K_D = (1.5 \pm 0.5)$ nM. The error bars (±0.1°) represent the reproducibility of the measurements of the angular minima

k_{diss}, as calculated by best fitting the kinetics of Fig. 2c, resulted in (2.8 ± 0.1) × 10^{-4} s^{-1}. As a consequence, the value of (2.5 ± 0.2) nM was found for K_D, in reasonable agreement with that found from the Langmuir isotherm fit.

Considering a weighted average value of K_D, namely 2.4 nM, it is worth noting that it is well within an order of magnitude of that (0.46 nM) measured for in vivo cells [15], which indicates a good mimetic action of the ganglioside incorporated into our ssBLM, at least for the GM1 recognition by CTB.

In addition to the 10 mol% GM1 concentration, the selective recruitment of CTB was demonstrated also for [GM1] = 2, 5, and 20 mol%, using a fixed CTB concentration (35 nM). The corresponding $\Delta\theta_{CTB}$ shifts vs the GM1 loadings are reported in Fig. 3.

At 10 mol% the angular shift $\Delta\theta_{CTB} = 0.47°$ pertains to a thickness of 3.6 nm, lower than that (4 nm) expected for a complete coverage of CTB in the typical side-on configuration [16]. At 20 mol% it reaches 0.62°, corresponding to 4.8 nm thickness. According to [17] this result indicates that part of the CTB units binds to GM1 in the edge-on configuration with the pentameric ring orthogonal to the surface, and therefore these CTB units do not exploit all the five pockets available for binding. Although the reason for the occurrence of this kind of linkage is not clear, a possible explanation is the availability of a restricted number of separated GM1 headgroups above the ssBLM, indeed a possible result of their clustering due to the ganglioside density [18, 19]. This phenomenon, observed even at 2.1 mol% GM1 concentration in a POPC ssBLM, [19] is further favoured in CerPCho/C ssBLM as recently demonstrated by MD simulations [20].

Binding of CTB to a lower number of sites is responsible for the weakening of the bond strength [7, 19], that can manifest itself in the increase of k_{diss} and/or a decrease of k_{ass}. Actually, a decrease in k_{ass} was accidentally found from the best exponential fit of the CTB association kinetics, reported in Fig. 2 ESM, that have been routinely recorded in order to monitor the stabilization of CTB adsorption on ssBLM:GM1. Indeed, the calculated k_{on} for the $GM1_{0.1}CerPCho_{0.5}C_{0.4}$ ssBLM (2.1 × 10^{-3} s^{-1}) is about two times higher than that (9.1 × 10^{-4} s^{-1}) obtained for $GM1_{0.2}CerPCho_{0.4}C_{0.4}$ ssBLM, confirming the presence of a weaker bonding of GM1 to CTB for higher GM1 loadings.

In summary, we have fabricated homogeneous and stable GM1-rich CerPCho/C ssBLM on plasmonic transducers, which allowed us to monitor the dissociation of CTB from GM1 embedded in a physiological-like solid supported environment. The measured value of K_D, 2.4 nM, is close to that found for in vivo cells, that indicates the potential of these systems as in vitro biomimicking

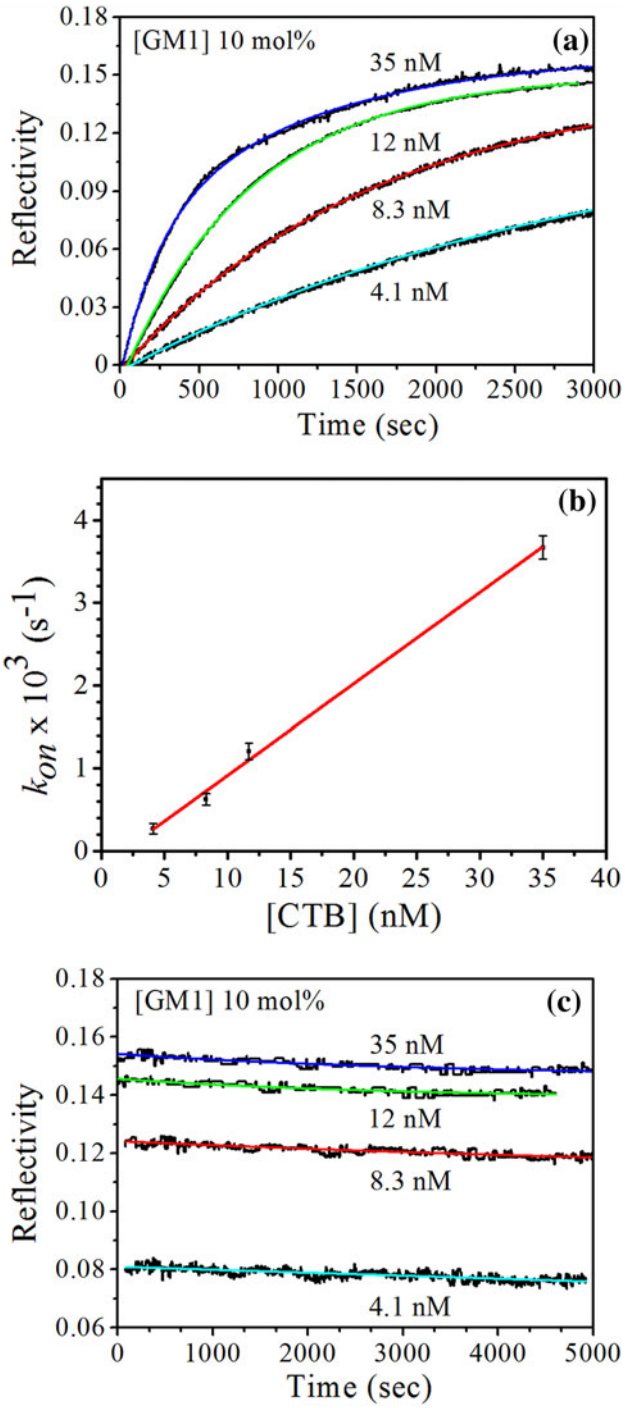

Fig. 2 **a** Experimental association kinetics of CTB to a ssBLM:GM1 (*black traces*) and their best fit (*colored lines* in the online version) at various concentrations in HBS (4.1, 8.3, 12, 35 nM). **b** Association rates and their experimental errors as calculated with the best fit procedure. The GM1 loading of the ssBLM is 10 mol%. *Straight line* linear best-fit, corresponding to an association constant k_{ass} = (1.10 ± 0.04) × 10^5 $M^{-1}s^{-1}$. **c** Dissociation kinetics (*black traces*) obtained contacting the ssBLM:GM1 to pure HBS. The superimposed exponential best fit curves are *colored* only in the online version. The resulting dissociation constant k_{diss} results (2.8 ± 0.1) × 10^{-4} s^{-1}

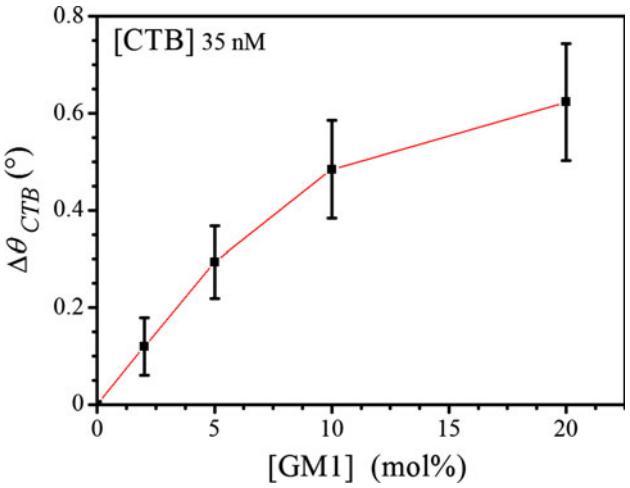

Fig. 3 Experimental steady angular shifts (*squares*) recorded after the incubation of a 35 nM CTB solution with ssBLM:GM1 at various GM1 loadings. *Vertical bars* are the reproducibility errors. The *line* (*red* in the online version) is a guide for the eye

platforms. In addition, whenever confirmed, the formation of GM1 clusters on these ssBLM will be a further benefit which could be fruitfully exploited to explore diseases, such as Alzheimer's disease, in which the clustering of GM1 plays a crucial key role [21].

Acknowledgments Drs. Davide Scarpellini and Paolo Paoli are gratefully acknowledged for their contribution to the fabrication and characterization of vesicles emulsions. Dr. Fabrizio Pieralli is acknowledged for the preparation of the plasmonic transducers. This work has been supported by the project "Coinvolgimento di *lipid rafts* in medicina molecolare" funded by Ente Cassa di Risparmio di Firenze (ECRF), Grant No 2010.0622.

References

1. Tsuji S, Arita M, Nagai Y (1983) GQ1b, a bioactive ganglioside that exhibits novel nerve growth factor (NGF)-like activities in the two neuroblastoma cell lines. J Biochem 94:303–306
2. Merritt EA, Kuhn P, Sarfaty S, Erbe JL, Holmes RK, Hol WG (1998) The 1.25 Å resolution refinement of the cholera toxin B-pentamer: evidence of peptide backbone strain at the receptor-binding site. J Mol Biol 282:1043–1059
3. Hooper NM (1998) Membrane biology: do glycolipid microdomains really exist? Curr Biol 8:114–116
4. Chini B, Parenti M (2004) G-protein coupled receptors in lipid rafts and caveolae: how, when and why do they go there? J Mol Endocrinol 32:325–338
5. Ostrom RS, Insel PA (2004) The evolving role of lipid rafts and caveolae in G protein-coupled receptor signalling: implications for molecular pharmacology. Br J Pharmacol 145:235–245
6. Simons K, Ikonen E (1997) Functional rafts in cell membranes. Nature 387:569–572
7. Kuziemko GM, Stroh M, Stevens RC (1996) Cholera toxin binding affinity and specificity for gangliosides determined by surface plasmon resonance. Biochemistry 35:6375–6384
8. Kakio A, Nishimoto S, Yanagisawa K, Kotsuzumi Y, Matsuzaki K (2001) Cholesterol dependent formation of GM1 ganglioside bound amyloid β-protein, an endogenous seed for Alzheimer amyloid. Biol Chem 276:24965–24990
9. Yuan C, Furlong J, Burgos P, Johnstone LJ (2002) The size of lipid rafts: an atomic force microscopy study of ganglioside GM1 domains in sphingomyelin/DOPC/Cholesterol membranes. Biophys J 82:2526–2535
10. Mao Y, Tero R, Imai Y, Hoshino T, Urisu T (2008) The morphology of $GM1_x/SM_{0.6-x}/Chol_{0.4}$ planar bilayers supported on SiO_2 surfaces. Chem Phys Lett 460:289–294
11. Margheri G, D'Agostino R, Becucci L, Guidelli R, Tiribilli B, Del Rosso M (2012) Surface plasmon resonance as detection tool for lipids lateral mobility in biomimetic membranes. Biomed Opt Express 3:3119–3126
12. Margheri G, D'Agostino R, Del Rosso M, Trigari S (2013) Fabrication of GM3-enriched sphingomyelin/cholesterol solid-supported lipid membranes on Au/SiO_2 plasmonic substrates. Lipids. doi:10.1007/s11745-013-3789-z
13. Salamon Z, Denavathan S, Alves ID, Tollin G (2005) Plasmon waveguide resonance studies of lateral segregation of lipids and proteins into microdomains (rafts) in solid supported bilayers. J Biol Chem 280:11175–11184
14. Edwards PR, Lowe PA, Leatherbarrow RJ (1997) Ligand loading at the surface of an optical biosensor and its effect upon the kinetics of protein–protein interactions. J Mol Recognit 10:128–134
15. Cuatrecasas P (1973) Cholera toxin-fat cell interaction and the mechanism of activation of the lipolytic response. Biochemistry 12:3567–3577
16. Cabral-Lilly D, Sosinsky GE, Reed RA, McDermott MR, Shipley GG (1994) Orientation of cholera toxin bound to model membranes. Biophys J 66:935–941
17. Terrettaz S, Stora T, Duschl C, Vogel H (1993) Protein binding to supported lipid membranes: investigation of the cholera toxin-ganglioside interaction by simultaneous impedance spectroscopy and surface plasmon resonance. Langmuir 9:1361–1369
18. Delmelle M, Dufrane SP, Brasseur R, Ruysschaert JM (1980) Clustering of gangliosides in phospholipid bilayers. FEBS Lett 121:11–14
19. Shi J, Yang T, Kataoka S, Zhang Y, Diaz AJ, Cremer PS (2007) GM1 clustering inhibits cholera toxin binding in supported phospholipid membranes. J Am Chem Soc 129:5954–5961
20. Mori K, Mahmood MI, Neya S, Matsuzaki K, Hoshino T (2012) Formation of GM1 ganglioside clusters on the lipid membrane containing sphingomyelin and cholesterol. J Phys Chem B 116:5111–5121
21. Kakio A, Nishimoto S, Yanagisawa K, Kozutsumi Y, Matsuzaki K (2002) Interaction of amyloid-β protein with various gangliosides in raft-like membranes: importance of GM1 ganglioside-bound form as an endogenous seed for Alzheimer amyloid. Biochemistry 41:7385–7390